

U-Load Dextramer®

Build multimers with your choice of peptide and peptide-receptive MHC I and MHC II alleles.



Chronically Elevated Levels of Short-Chain Fatty Acids Induce T Cell–Mediated Ureteritis and Hydronephrosis

This information is current as of February 26, 2022.

Jeongho Park, Craig J. Goergen, Harm HogenEsch and Chang H. Kim

J Immunol 2016; 196:2388-2400; Prepublished online 27 January 2016;

doi: 10.4049/jimmunol.1502046

<http://www.jimmunol.org/content/196/5/2388>

Supplementary Material <http://www.jimmunol.org/content/suppl/2016/01/26/jimmunol.1502046.DCSupplemental>

References This article **cites 53 articles**, 18 of which you can access for free at: <http://www.jimmunol.org/content/196/5/2388.full#ref-list-1>

Why *The JI*? [Submit online.](#)

- **Rapid Reviews! 30 days*** from submission to initial decision
- **No Triage!** Every submission reviewed by practicing scientists
- **Fast Publication!** 4 weeks from acceptance to publication

**average*

Subscription Information about subscribing to *The Journal of Immunology* is online at: <http://jimmunol.org/subscription>

Permissions Submit copyright permission requests at: <http://www.aai.org/About/Publications/JI/copyright.html>

Email Alerts Receive free email-alerts when new articles cite this article. Sign up at: <http://jimmunol.org/alerts>



Chronically Elevated Levels of Short-Chain Fatty Acids Induce T Cell–Mediated Ureteritis and Hydronephrosis

Jeongho Park,* Craig J. Goergen,^{†,‡} Harm HogenEsch,* and Chang H. Kim*,^{†,‡}

Short-chain fatty acids (SCFAs) are major products of gut microbial fermentation and profoundly affect host health and disease. SCFAs generate IL-10⁺ regulatory T cells, which may promote immune tolerance. However, SCFAs can also induce Th1 and Th17 cells upon immunological challenges and, therefore, also have the potential to induce inflammatory responses. Because of the seemingly paradoxical SCFA activities in regulating T cells, we investigated, in depth, the impact of elevated SCFA levels on T cells and tissue inflammation in mice. Orally administered SCFAs induced effector (Th1 and Th17) and regulatory T cells in ureter and kidney tissues, and they induced T cell–mediated ureteritis, leading to kidney hydronephrosis (hereafter called acetate-induced renal disease, or C2RD). Kidney hydronephrosis in C2RD was caused by ureteral obstruction, which was, in turn, induced by SCFA-induced inflammation in the ureteropelvic junction and proximal ureter. Oral administration of all major SCFAs, such as acetate, propionate, and butyrate, induced the disease. We found that C2RD development is dependent on mammalian target of rapamycin activation, T cell–derived inflammatory cytokines such as IFN- γ and IL-17, and gut microbiota. Young or male animals were more susceptible than old or female animals, respectively. However, SCFA receptor (GPR41 or GPR43) deficiency did not affect C2RD development. Thus, SCFAs, when systemically administered at levels higher than physiological levels, cause dysregulated T cell responses and tissue inflammation in the renal system. The results provide insights into the immunological and pathological effects of chronically elevated SCFAs. *The Journal of Immunology*, 2016, 196: 2388–2400.

Gut microbiota produce large amounts of metabolites from metabolism of dietary materials, host secretions, and microbial products. Short-chain fatty acids (SCFAs), such as acetate (C2), propionate (C3), and butyrate (C4), are the most abundantly produced microbial metabolites in the gut (1). Digestion-resistant dietary fibers and glycosylated mucins are the main source of gut luminal SCFAs. SCFAs fuel host cells (2) and regulate obesity (3), blood pressure (4), and the immune system (5). Certain functions of SCFAs are mediated by cell surface G protein–coupled receptors (GPCRs) such as GPR41, GPR43, GPR109A, and Olfr78 (4, 6, 7). Many functions of SCFAs, however, are mediated in a GPCR-independent manner. Some of the GPCR-independent functions are mediated, in part, by their

effect on cellular metabolism (8, 9). SCFAs are histone deacetylase (HDAC) inhibitors and, therefore, regulate gene expression and protein functions (5, 10, 11).

SCFAs induce IL-10–expressing Foxp3⁺ and Foxp3[–] regulatory T cells (5, 10–12). These effects may account for certain beneficial effects of SCFAs on tissue inflammation (13–15). However, SCFAs can also induce effector T cells such as Th1 and Th17 cells, which fight pathogens during infection and mediate inflammatory responses (5). Moreover, SCFAs affect the cytokine production phenotype of dendritic cells for both tolerogenic and inflammatory responses (16, 17). Thus, the functions of SCFAs in regulating immune cells, including T cells, appear complex. Moreover, the impact of elevated SCFA levels on tissue inflammation remains to be investigated.

To closely determine the effect of elevated SCFA levels on tissue inflammation, we performed a series of experiments with mice orally administered with SCFAs. We found that chronically elevated levels of SCFAs induce a T cell–mediated renal disease with progressive ureteritis and hydronephrosis (hereafter called acetate- or C2-induced renal disease, or C2RD). C2RD is caused, in part, by excessive mammalian target of rapamycin (mTOR) activation and generation of inflammatory Th1 and Th17 cells in the ureteropelvic junction (UPJ) and the proximal part of the ureter. Our findings demonstrate the potentially inflammatory activity of chronically elevated SCFAs in the renal system.

Materials and Methods

Mice and treatments

C57BL/6 mice (originally from Harlan Laboratories, Indianapolis, IN), *Gpr43*^{–/–} mice (Deltagen, San Mateo, CA), *Gpr41*^{–/–} mice (provided by M. Yanagisawa, University of Texas Southwestern Medical Center, Dallas, TX), and TCR β -deficient mice (B6.129P2-*Tcrb*^{tm1Mom}/J, The Jackson Laboratory) were kept at Purdue University for at least 12 mo before use. Mice were treated with sodium acetate (C2 at 100, 150, or 200 mM [pH 7.5]), sodium propionate (C3 at 200 mM [pH 7.5]), or sodium butyrate (C4 at 200 mM [pH 7.5]) in drinking water from 3 wk of age for 2–6 wk. When indicated, mice were treated with rapamycin (25 μ g/ml, LC Laboratories)

*Laboratory of Immunology and Hematopoiesis, Department of Comparative Pathobiology, Purdue University, West Lafayette, IN 47907; [†]Weldon School of Biomedical Engineering, Purdue University, West Lafayette, IN 47907; and [‡]Purdue Center for Cancer Research, Purdue University, West Lafayette, IN 47907

ORCID: 0000-0002-0340-9181 (J.P.); 0000-0001-8883-7953 (C.J.G.); 0000-0002-2738-9189 (H.H.); 0000-0003-4618-9134 (C.H.K.).

Received for publication September 16, 2015. Accepted for publication December 31, 2015.

This work was supported in part by National Institutes of Health Grants R01AI074745, R01DK076616, R01AI080769, and 1S10RR028293, and by a grant from the National Multiple Sclerosis Society (to C.H.K.).

The array data presented in this article have been submitted to the National Center for Biotechnology Information's Gene Expression Omnibus database (<http://www.ncbi.nlm.nih.gov/geo/>) under accession number GSE69864.

Address correspondence and reprint requests to Dr. Chang H. Kim, Purdue University, 725 Harrison Street, VPTH 126, West Lafayette, IN 47907. E-mail address: chkim@purdue.edu

The online version of this article contains supplemental material.

Abbreviations used in this article: C2, acetate; C3, propionate; C4, butyrate; C2RD, acetate- or C2-induced renal disease; GPCR, G protein–coupled receptor; h, human; HDAC, histone deacetylase; m, murine; mTOR, mammalian target of rapamycin; PKD, polycystic kidney disease; qRT-PCR, quantitative real-time PCR; SCFA, short-chain fatty acid; UPJ, ureteropelvic junction; UUO, unilateral ureteral obstruction.

Copyright © 2016 by The American Association of Immunologists, Inc. 0022-1767/16/\$30.00

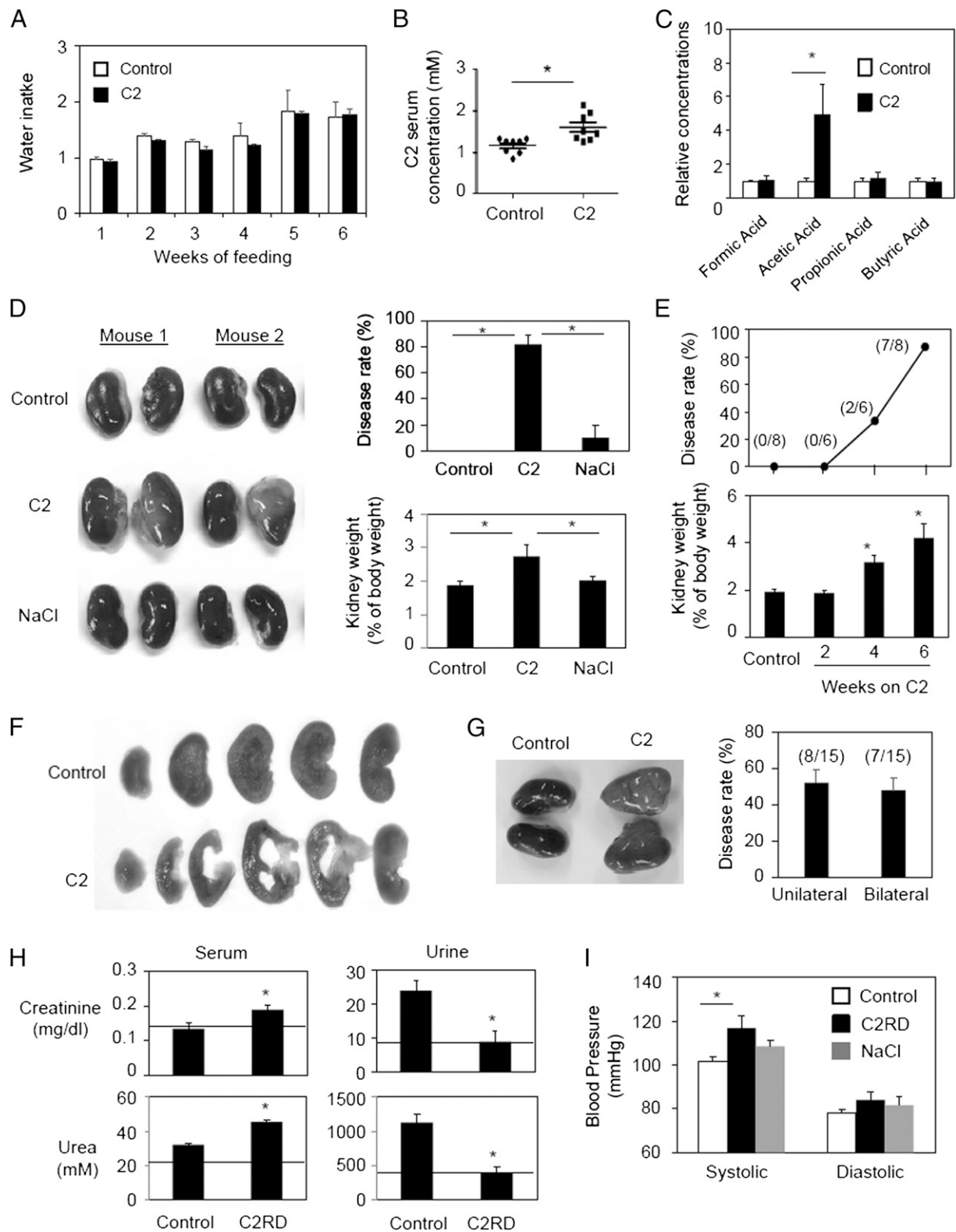


FIGURE 1. Oral administration of C2 induces a renal disease (C2RD). **(A)** Weekly water intake (ml/g body weight) was measured for the control and C2 water groups. **(B)** Concentrations of SCFAs in blood after oral C2 administration via drinking water for 6 wk. **(C)** Concentrations of SCFAs in kidney tissues after C2 feeding. **(D)** Oral administration of C2 (200 mM) for 6-wk-induced hydronephrosis. C2 or NaCl (200 mM) was administered in drinking water. Percentage disease (hydronephrosis) rate and relative kidney weight are shown. **(E)** Kinetics of C2RD development during a 6-wk period. The control group was on regular water for 6 wk. **(F)** Cross sections of control and C2RD kidney tissues. **(G)** Unilateral versus bilateral occurrence of C2RD. **(H)** Serum and urine concentrations of creatinine and urea in C2RD. **(I)** Blood pressure in control and C2RD mice. Mice were examined after C2 administration from 3 to 9 wk of age. Representative or pooled data are shown [$n = 8-10$ for **(A)** and **(B)**; $n = 4$ for **(C)**; $n = 6-15$ for **(D)**, **(E)**, **(G)**, and **(H)**; $n = 5$ for **(I)**]. Error bars are SEM. * $p \leq 0.05$ from control group by Mann-Whitney U test (**B**) or Student t test (**C-E** and **G-I**).

and/or vancomycin (0.5 g/l) in drinking water for same time periods. Some mice were treated from 32 wk of age with SCFAs. C2RD diagnosis was made after sacrifice based on hydronephrosis in kidneys. Male mice were used for most experiments unless indicated otherwise. Mice were treated also with Abs to IL-17A (clone 17F3, Bio X Cell) or IFN- γ (clone XMG1.2, Bio X Cell) (100 μ g/mouse, i.p. once a week) for 6 wk. All animal experiments were approved by the Purdue Animal Care and Use Committee.

Confocal microscopy and histology

Frozen sections of kidneys or ureters (8 μ m) were fixed with acetone and stained with rabbit polyclonal Ab to collagen type IV (Acris Antibodies) and then stained with fluorescently labeled polyclonal anti-rabbit IgG Abs and Abs to CD4 (clone RM 4-5), CD11c (clone N418), Gr-1 (clone RB6-8C5), cytokeratin (clone AE1/AE3), and muscle actin (clone HHF35). Fluorescent confocal images of kidney and ureter tissues were acquired with a Leica SP5 II laser scanning confocal microscope. For histological analysis, paraffin tissue sections (8 μ m) were stained with H&E.

Serum and urine analysis

Creatinine concentration in serum and urine was determined as described before (18). Briefly, 1 ml creatinine assay solution composed of picric acid, sodium hydroxide, and EDTA disodium salt was mixed with 0.1 ml standard solutions, serum, or urine. Absorbance at 492 nm was measured at 30 and 90 s later. For urea concentration, serum, urine, or standard solutions were reacted with 200 μ l mixed acid solution (H_2SO_4 , H_3PO_4 , and H_2O in a ratio of 1:3:7) and 10 μ l 9% α -isonitrosopropiophenone solution. The mixtures were reacted for 30 s at 95°C and absorbance at 540 nm was measured. Creatinine and urea concentrations were calculated based on the absorbance values of standard solutions.

Blood pressure

Systolic and diastolic blood pressures were noninvasively measured by determining the tail blood volume with a volume pressure recording sensor and an occlusion tail cuff (CODA System, Kent Scientific, Torrington, CT) (19). Maximum cuff pressure was set to 250 mm Hg, with 20 s for each inflation run as per the manufacturer's recommendations. Each mouse was measured 20 times and averages of all accepted runs were used.

Cell culture and flow cytometry

Total renal lymph node cells were obtained by digesting lymph node tissues with collagenase type 3 (Worthington Biochemical, Lakewood NJ) at 37°C for 30 min and cultured on coated anti-CD3 (5 μ g/ml, clone 145-2C11) in several different culture conditions: human (h)IL-2 (100 U/ml) for a Tnp condition; hIL-2, murine (m)IL-12 (1 ng/ml), and anti-mIL4 (clone 11B11, 10 μ g/ml) for a Th1 condition; hTGF- β 1 (5 ng/ml), mIL-6 (20 ng/ml), mIL-1 β (10 ng/ml), mIL-23 (10 ng/ml), mIL-21 (10 ng/ml), mTNF- α (20 ng/ml), anti-mIL-4 (10 μ g/ml, clone 11B11), and anti-mIFN- γ (10 μ g/ml, clone XMG1.2) for a Th17 condition. The cells were cultured with SCFAs (C2, 10 mM; C3, 1 mM; C4, 0.5 mM) and/or rapamycin (25 nM, Enzo Life Sciences) for 3 d for mTOR activation or 5 d for cytokine expression. For flow cytometry, kidney or ureter tissues were digested with collagenase type 3 for 60 min. For intracellular staining of IL-10, IL-17, and IFN- γ , cells were stained with anti-CD4 and then activated in RPMI 1640 (10% FBS) with 12-myristate

13-acetate (50 ng/ml), ionomycin (1 μ M), and monensin (2 mM) for 4 h. Cells were then fixed, permeabilized, and stained with Abs to IL-10 (clone JES5-16E3), IL-17A (clone TC11-18H10.1), IFN- γ (clone XMG1.2), and/or anti-Foxp3 (clone FJK-16s). An Ab to phosphorylated rS6 (clone Ser235/236; D57.2.2E) was used to determine rS6 protein phosphorylation. Flow cytometry was performed with a FACSCanto II instrument (BD Biosciences) with FACSDiva or FlowJo software. The frequencies of T helper cells were obtained from the total lymphocyte and CD4⁺ gates. The total cell numbers were obtained based on frequencies of each cell population and numbers of retrieved cells from each organ (one spleen, two draining lymph nodes, one kidney, and two ureters).

Measurements of SCFA levels in kidney tissues

Kidney tissues (100 mg) were homogenized in 900 μ l water and 1.4-mm ceramic beads using a Precellys 24 homogenizer. Tissue homogenates were labeled and analyzed with an Agilent 6460 triple quad liquid chromatography/mass spectrometry system (Agilent Technologies) as described before (5). Sample SCFA concentrations were determined based on peak areas of the internal and external standards.

Microarray and quantitative real-time PCR

RNA, isolated from C2RD kidneys after 6 wk of oral administration, was hybridized to mouse 430 2.0 chips (Affymetrix). The data were processed as described previously (20). The array data have been deposited in the Gene Expression Omnibus database (<http://www.ncbi.nlm.nih.gov/geo/> accession no. GSE69864). The GenePattern genomic analysis platform (<http://www.broad.mit.edu/cancer/software/genepattern/>), Cluster 3.0, and TreeView 1.6 (Eisen Laboratory, <http://rana.lbl.gov/EisenSoftware.htm>) were used to visualize the data. Published gene expression data were retrieved from the Gene Expression Omnibus site: GSE36496 (unilateral ureteral obstruction [UUO]), GSE48041 (*Mgb*^{-/-}), GSE12024 (lupus), and GSE24352 (polycystic kidney disease [PKD]). Gene IDs were converted into Agilent ID using DAVID Bioinformatics Resources 6.7 (<http://david.abcc.ncifcrf.gov>) for comparative analysis of the data obtained with different microarray platforms. For quantitative real-time PCR (qRT-PCR), total RNA was extracted with TRIzol solution (Invitrogen), and cDNA was synthesized with SuperScript II reverse transcriptase (Invitrogen). qRT-PCR was performed with Maxima SYBR Green/ROX quantitative PCR master mix (Thermo Scientific). The primers used for qRT-PCR are listed in Supplemental Table I. Expression levels of genes were normalized by β -actin levels.

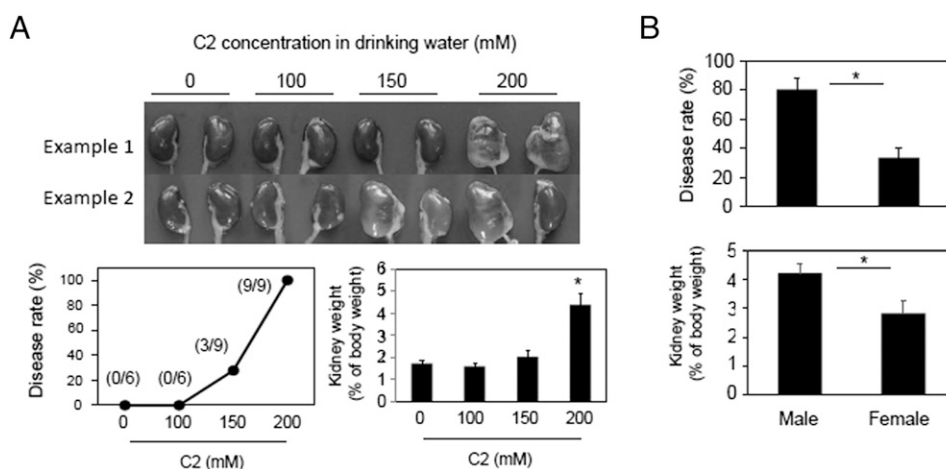
Bacterial DNA analysis

Bacterial DNA was isolated from cecal content using the FastDNA SPIN Kit (MP Biomedicals) according to the manufacturer's protocol. Quantitative PCR was performed with primers described before (15, 21). Differences (Δ CT) between cycle threshold (C_T) values of eubacteria and specific bacterial groups were used to obtain normalized levels of each bacterial group ($2^{-\Delta CT}$). Relative abundance of each bacterial group in C2RD was obtained after normalization with that of control groups.

Statistical analysis

A Student *t* test (one- or two-tailed) or Mann-Whitney *U* test was used to determine the significance of differences between two groups. A *p* value ≤ 0.05 was considered significant.

FIGURE 2. Dose-dependent and sex-biased development of C2RD. (A) Mice were orally administered with C2 at indicated concentrations in drinking water for 6 wk. Gross appearance, disease rate, and relative kidney weight are shown. (B) Male and female mice were compared for C2RD development. C2 (200 mM) was orally administered for 6 wk. Representative or pooled data are shown [$n = 6$ –9 for (A), $n = 14$ for (B)]. Error bars are SEM. * $p \leq 0.05$ from control group by Student *t* test (paired two-tailed).



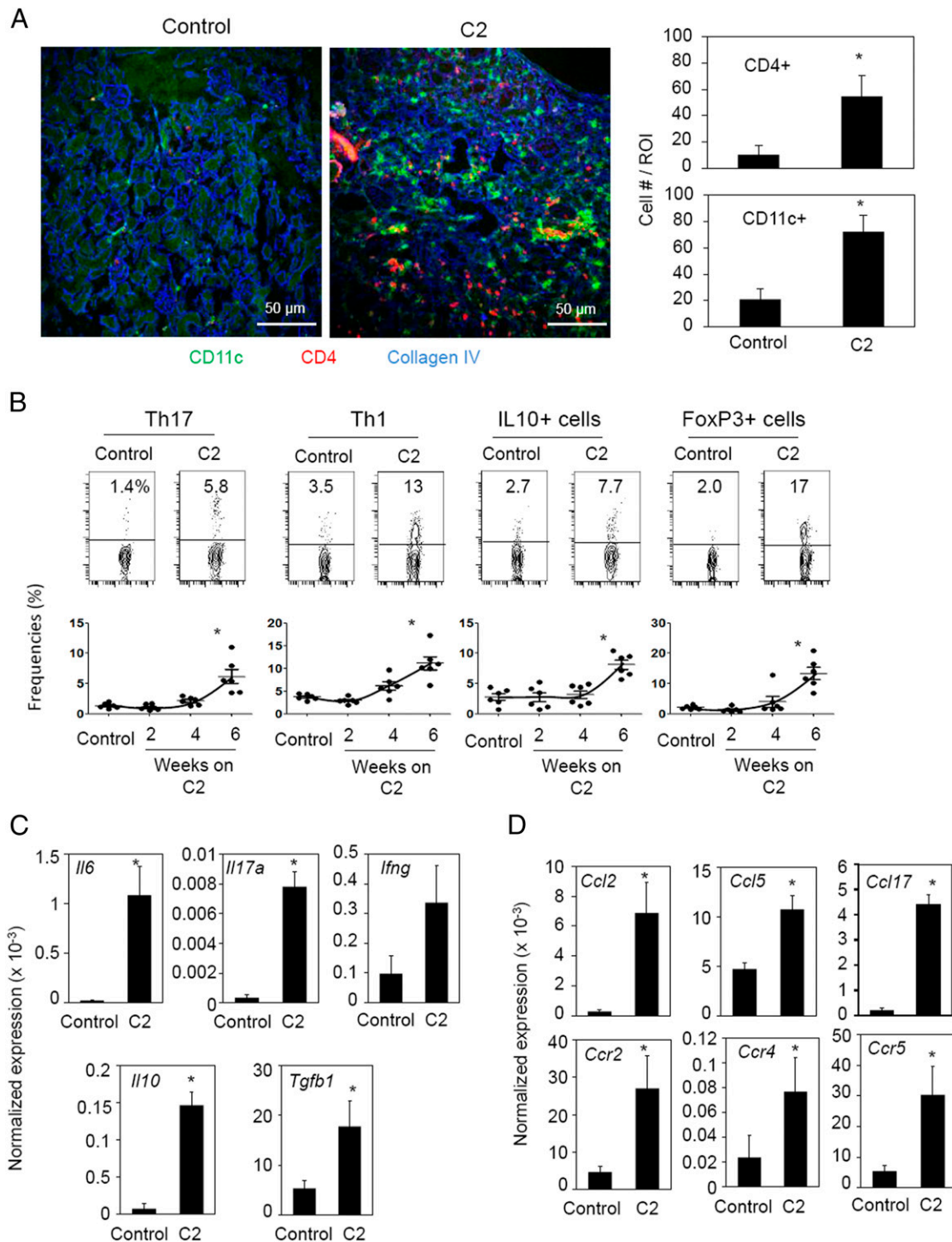


FIGURE 3. Changes in effector and regulatory T cells in C2RD kidney tissues. **(A)** Confocal analysis of kidney tissues for infiltration by CD4⁺ T cells and CD11c⁺ cells. **(B)** Changes in the frequencies of effector (Th17 and Th1) and regulatory (IL-10⁺ and Foxp3⁺) T cells. The flow data were gated for CD4⁺ T cells in affected kidneys during the course of C2RD development. The control group was on regular water for 6 wk. Flow cytometry for indicated CD4⁺ T subsets in affected kidney tissues was performed. Expression of cytokines **(C)** and chemokines and chemokine receptors **(D)** expressed in affected kidneys in C2RD is shown. qRT-PCR was performed. Representative or pooled data are shown [$n = 6$ for (A) and (B), $n = 3-6$ for (C) and (D)]. Error bars are SEM. * $p \leq 0.05$ from control groups by Student t test (paired two-tailed).

Results

Oral administration of C2 induces a progressing renal disease

SCFAs are absorbed through the gut epithelium and transported to the renal system via the bloodstream. The C2 level is on average ~ 130 mM in the human colon and ranges from 80 to 400 μ M in the blood (1). To determine the effect of elevated SCFA levels

on the renal system, we performed oral administration of C2 (sodium acetate at 200 mM) in drinking water for 6 wk. There was no difference in water intake between the regular and C2 groups (Fig. 1A). C2 concentration was increased by $\sim 50\%$ in gut lumen (5) and blood (Fig. 1B) but increased $\sim 400\%$ in kidney tissues (Fig. 1C) after C2 administration for 6 wk. C2 concentrations in

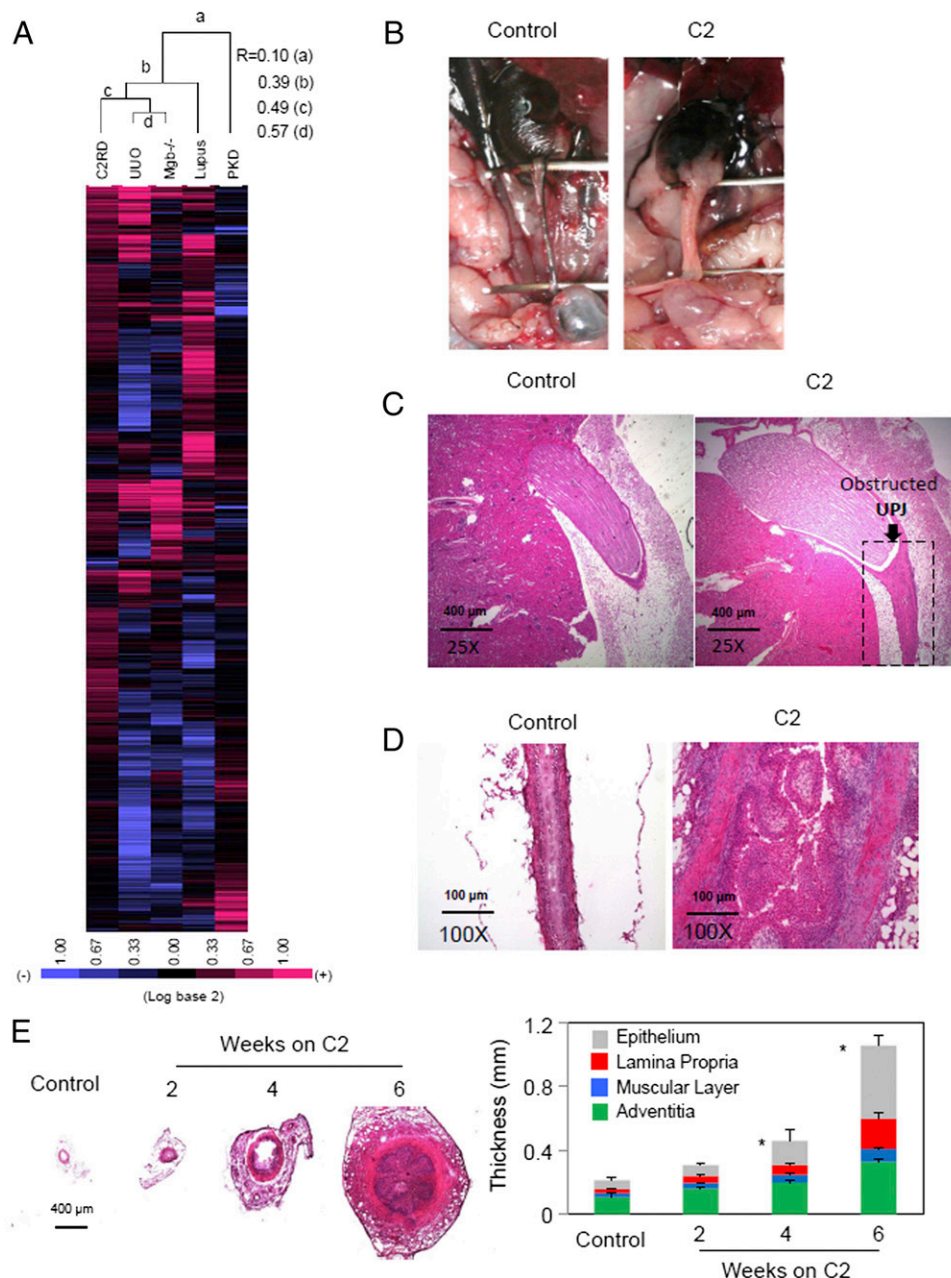


FIGURE 4. C2RD accompanies inflammation and hyperplasia in ureters. **(A)** Comparative transcriptome analysis among UUO, *Mgb*^{-/-} congenital obstructive nephropathy, lupus nephritis, and PKD. Two separate microarray data sets for C2RD were combined for comparison with published transcriptome data in the Gene Expression Omnibus database. The analysis included 9144 genes significantly expressed in C2RD tissues. **(B)** India ink test of ureteral obstruction. **(C)** Histological analysis of UPJ in control and C2RD mice. **(D)** Longitudinal tissue sections of affected proximal ureters. **(E)** Thickness changes in the proximal ureter over time during C2RD pathogenesis. The control group was on regular water for 6 wk. H&E staining was performed in (C), (D), and (E). Original magnification $\times 25$ (C and E) and $\times 100$ (D). Representative or pooled data are shown [$n = 4-5$ for (E)]. Error bars are SEM.

control and C2RD kidney tissues were 0.56 ± 0.079 and 2.78 ± 1.02 mM, respectively (Fig. 1C). We sacrificed mice 6 wk after the oral administration of C2 water and found that C2-fed mice unexpectedly developed a renal disease, which we termed C2RD (Fig. 1D). The kidneys had severe swelling with hydronephrosis. Complete loss of kidney cortex and medulla occurred in many mice with severe C2RD. This was not due to increased levels of sodium (Na^+) ion because administration of sodium chloride (NaCl) at the same concentration hardly induced the disease (Fig. 1D). C2RD was detected in some mice just after 4 wk, and most mice were affected at 6 wk of the treatment (Fig. 1E). Dilated renal pelvis and compressed medulla and cortex were ap-

parent in sectioned kidney tissues (Fig. 1F). In $\sim 45\%$ of the mice, both kidneys developed hydronephrosis (Fig. 1G). Creatinine and urea levels were significantly increased in the serum, whereas the concentrations of these metabolites in urine were reduced (Fig. 1H), indicating decreased kidney function in C2RD. Also increased in C2RD was systolic blood pressure (Fig. 1I), which is frequently associated with decreased kidney function (22).

C2RD development occurred in some mice administered with C2 at 150 mM but not 100 mM, indicating that this is a dose-dependent response (Fig. 2A). Additionally, male mice were more susceptible to C2RD than were female mice (Fig. 2B), which is reminiscent of the sex differences in human chronic kidney diseases (23). Histo-

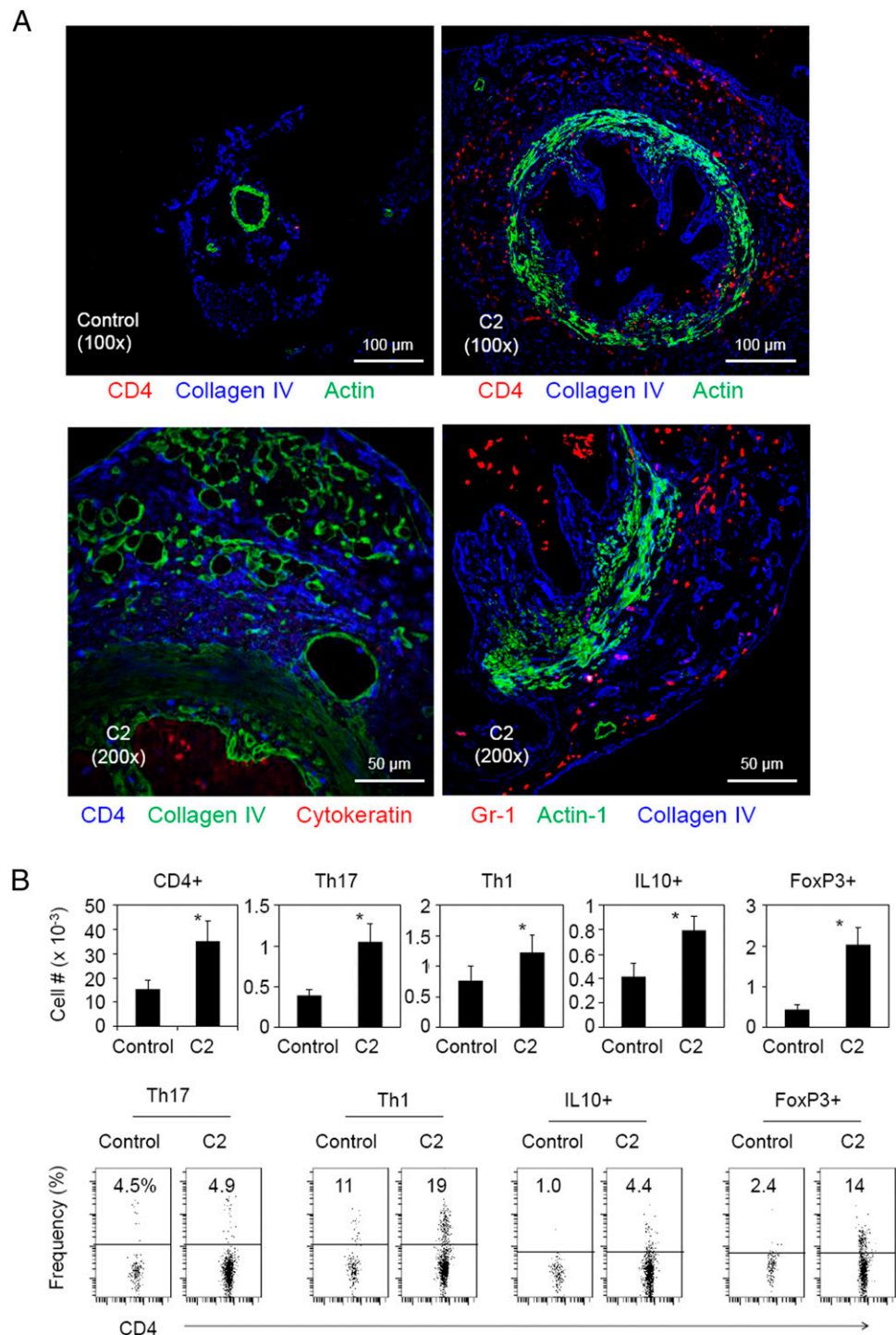


FIGURE 5. Effector and regulatory T cells infiltrate ureteral tissues in C2RD. **(A)** Immunohistochemistry of proximal ureter tissues. Abs to CD4, Gr-1, muscle actin (smooth muscle cells), cytokeratin (epithelial cells), and/or collagen IV were used. **(B)** Numbers and frequencies of Th17, Th1, IL-10⁺, and Foxp3⁺ CD4⁺ T cells in ureters of C2RD and control mice. The flow data were gated for CD4⁺ T cells. Mice were examined after C2 administration for 6 wk from 3 wk of age. Representative or pooled data are shown [$n = 6$ for (B)]. Error bars are SEM. * $p \leq 0.05$ from control groups by Student t test (paired two-tailed).

logical analysis revealed inflammation and varied loss of the renal medulla and the cortex (Supplemental Fig. 1A). The UPJ was greatly thickened with marked epithelial and smooth muscle hyperplasia and immune cell infiltration (Supplemental Fig. 1B).

Increased inflammatory Th17 and Th1 cells in C2RD

Immunohistochemistry revealed that CD4⁺ T cells and CD11c⁺ cells were increased broadly in affected kidney tissues (Fig. 3A). Because of the increased CD4⁺ T cells in affected kidney tissues, we examined more closely the inflammatory and suppressive cytokines expressed by infiltrating CD4⁺ T cells. The frequencies of Th17 and Th1 cells were increased in C2RD kidney tissues (Fig. 3B). Regulatory T cells such as IL-10⁺ cells and Foxp3⁺

T cells were also increased in C2RD. The increases of kidney Th17, Th1, IL-10⁺, and Foxp3⁺ T cells started already at ~4 wk (Fig. 3B). Kidney-draining lymph nodes were greatly expanded in C2RD (Supplemental Fig. 2A), indicating lymphocyte activation. The frequencies and numbers of the Th cell subsets were increased in kidneys, ureters, and draining renal lymph nodes but not in spleen (Supplemental Fig. 2B, 2C). Inflammatory cytokines and chemokines activate tissue cells and recruit immune cells for tissue inflammation and fibrosis in the renal system (24, 25). The expression of *Il6*, *Il17a*, *Ifng*, *Ccl2*, *Ccl5*, and *Ccl17* mRNA was greatly increased in affected kidney tissues (Fig. 3C, 3D). The expression of *Il10* (a regulatory cytokine) and *Tgfb1* (a regulatory and fibrosis-related cytokine) mRNA was also increased.

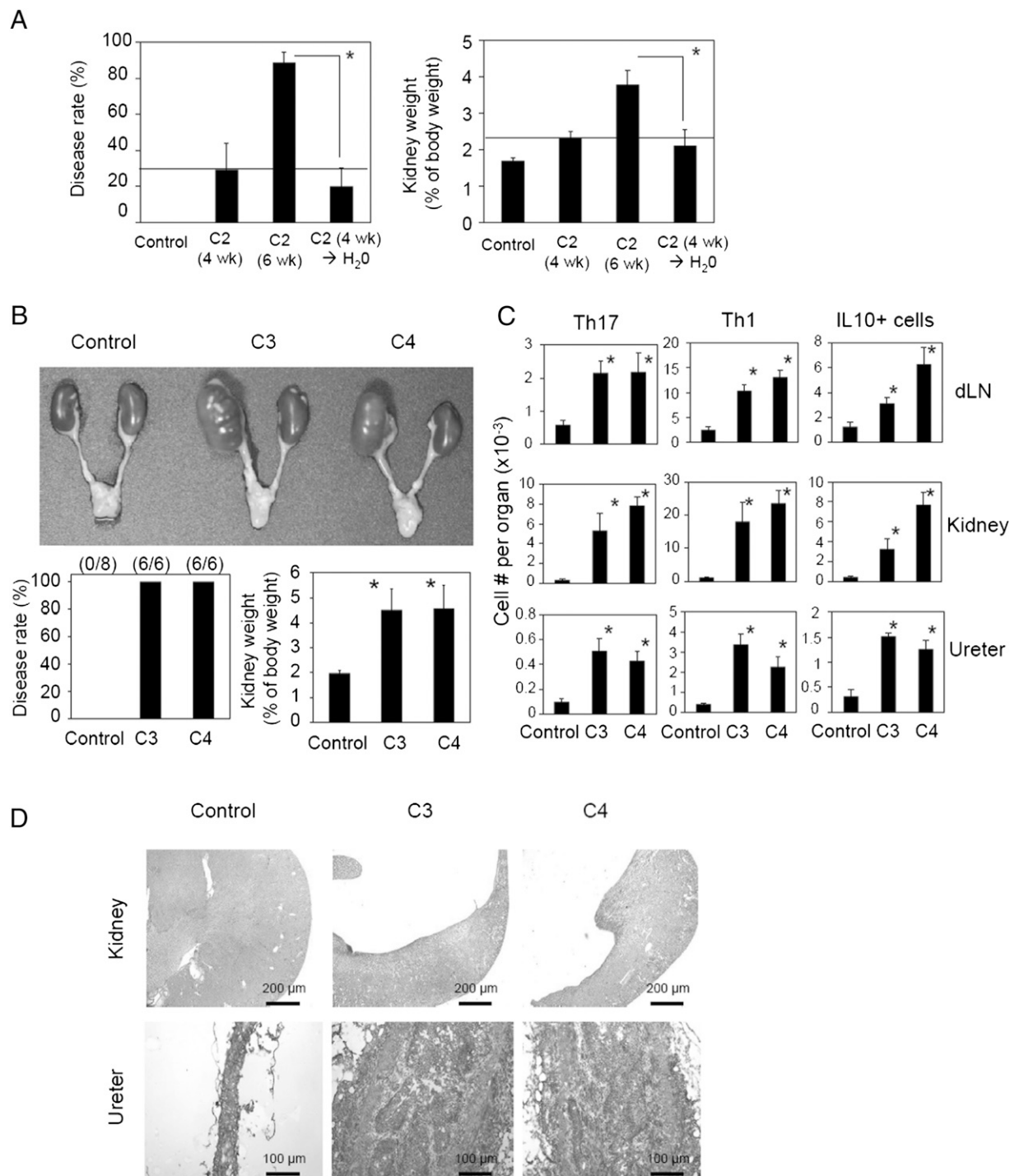


FIGURE 6. Effective C2RD development requires prolonged exposure to C2, and the disease is also induced by C3 and C4. **(A)** Mice were fed C2 water for 4 wk and then with regular or C2 water for 2 additional weeks. Gross tissue appearance, disease rate, and relative kidney weight are shown. **(B)** C2RD-like kidney disease in the mice fed with C3 or C4 for 6 wk. **(C)** Numbers of Th17, Th1, and IL-10⁺ CD4⁺ T cells in affected draining lymph nodes (dLN), kidneys, and ureters of control and C2RD mice. **(D)** Histological analysis of kidney and ureter tissues. Representative or pooled data are shown [$n = 6-18$ for (A)–(C)]. Mice were fed with SCFA water from 3 to 9 wk of age. Error bars are SEM. Original magnification $\times 50$ (kidney) and $\times 100$ (ureter) (D). $*p \leq 0.05$ from control groups by Student t test.

C2RD has a gene expression pattern consistent with tissue inflammation, fibrosis, and hyperplasia

The results so far indicate that C2RD has a pathological feature consistent with inflammatory renal diseases in animals and humans. To determine the relationship of C2RD to other renal diseases at global transcriptome level, we performed a microarray study. We compared our C2RD data with published transcriptome

data obtained with UUO, congenital obstructive nephropathy in megabladder (*Mgb*)^{-/-} male, lupus nephritis, and embryonic PKD models (26–29). In global gene expression, C2RD was more related to the renal disease models induced by ureteral obstruction (UUO and *Mgb*^{-/-}) and lupus nephritis than the embryonic PKD model (Fig. 4A). The similarity of C2RD to ureteral obstruction models was also clear in the expression of genes related to tissue

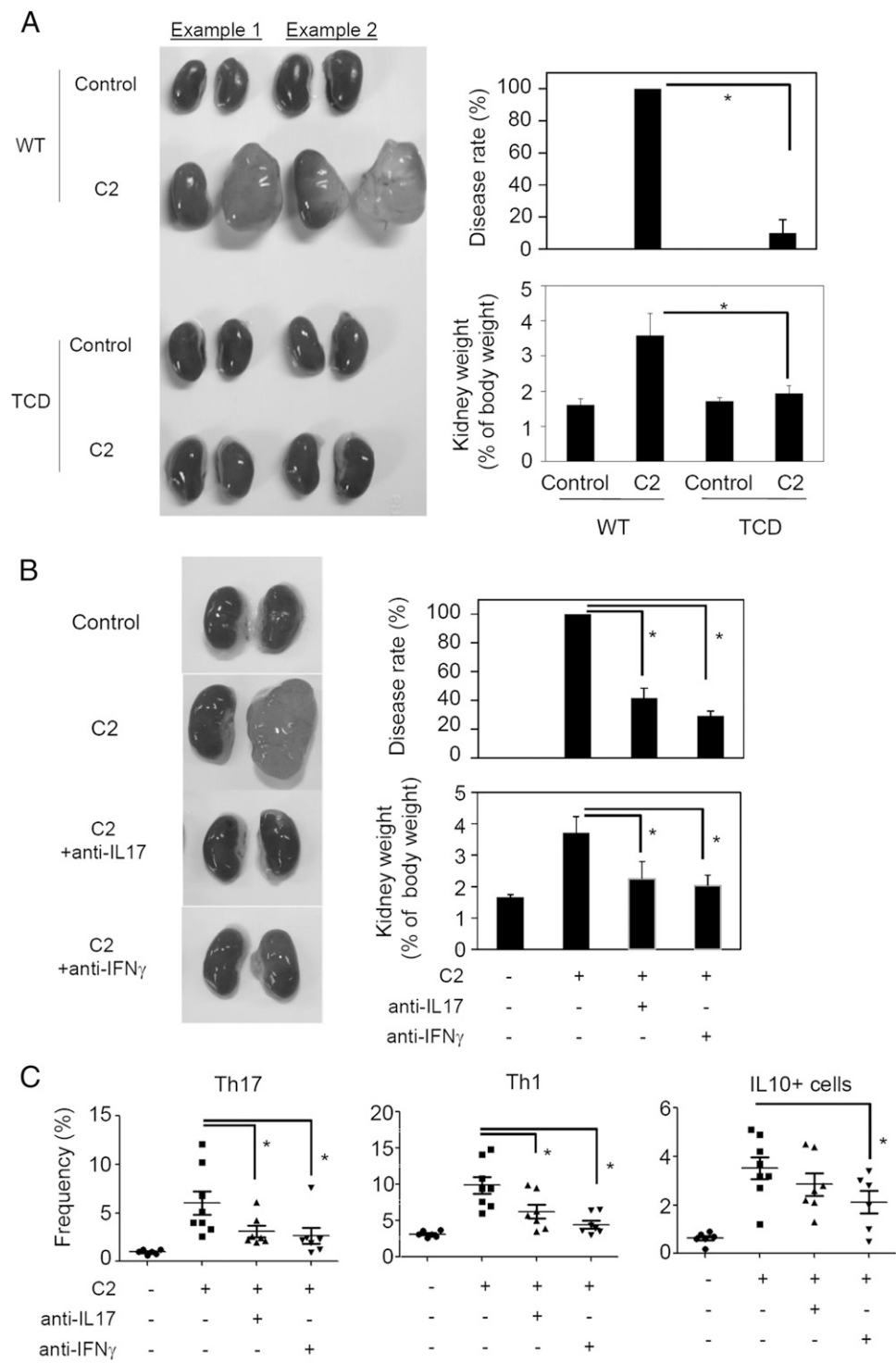


FIGURE 7. Roles of T cells and inflammatory cytokines in C2RD development. **(A)** Gross kidney appearance, disease rate, and relative kidney weight of wild-type (WT) and T cell (α -TCR)-deficient (TCD) mice fed with C2 for 6 wk. **(B)** Blocking IL-17A and IFN- γ effectively suppressed C2RD. Gross appearance of kidneys, C2RD rate, and relative kidney weight are shown. **(C)** Frequencies of Th17, Th1, and IL-10 $^{+}$ CD4 $^{+}$ T cells in kidneys. Mice were fed with C2 water from 3 to 9 wk of age. Representative or pooled data are shown [$n = 6$ –8 for (A)–(C)]. Error bars are SEM. $*p \leq 0.05$ by Student t test.

inflammation, fibrosis, NO, growth factors and receptors, and cell proliferation pathways (Supplemental Fig. 3).

Ureter inflammation, hyperplasia, and obstruction in C2RD

Because of the hydronephrosis-like appearance and global gene expression pattern related to ureter obstruction models, we performed a ureter function test with India ink injection into the renal pelvis and found that affected ureters were completely blocked

(Fig. 4B). UPJ and renal papillae tissues were expanded with tissue hyperplasia and obstruction (Fig. 4C). Lamina propria, muscular layer, and adventitia layers in the proximal ureter area were all greatly expanded (Fig. 4D). At 6 wk of C2 treatment, the proximal ureter was expanded up to ~ 10 -fold the diameter of control mouse ureters (Fig. 4E). Mild epithelial and smooth muscle cell hyperplasia were detected in the proximal ureter even at 2 wk of C2 administration (Fig. 4E). Immunohistochemistry

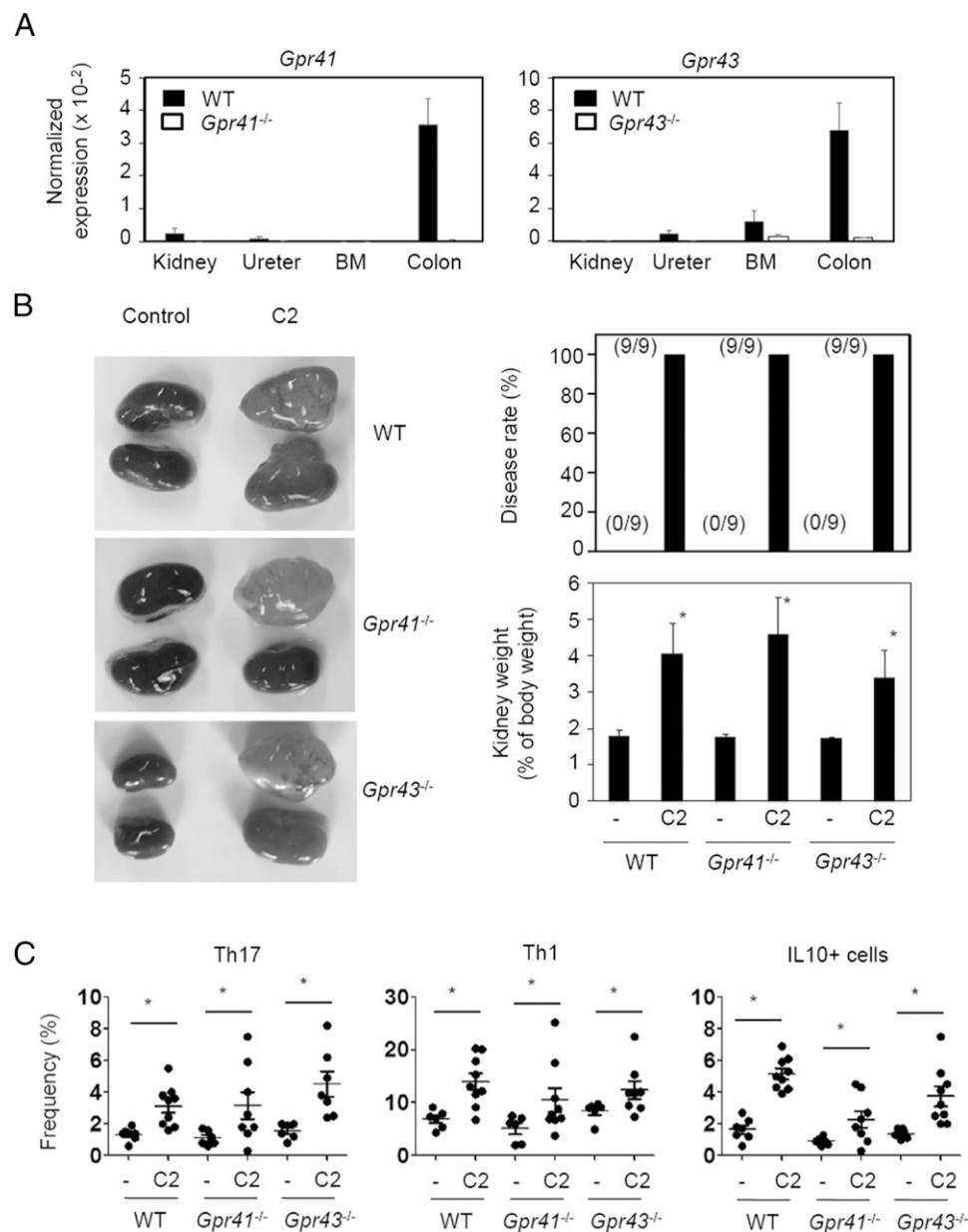


FIGURE 8. $Gpr41^{-/-}$ and $Gpr43^{-/-}$ mice develop C2RD. **(A)** Expression levels of $Gpr41$ and $Gpr43$. **(B)** C2RD development in wild-type (WT), $Gpr41^{-/-}$, and $Gpr43^{-/-}$ mice. Gross appearance, C2RD rate, and kidney weight after oral administration with C2 for 6 wk are shown. **(C)** Changes in Th1, Th17, and IL-10⁺ T cells in indicated mice. The flow data were gated for CD4⁺ T cells. Mice were fed with C2 water from 3 to 9 wk of age. Error bars are SEM. * $p \leq 0.05$ from control groups by Student t test [paired two-tailed; $n = 3$ for (A), $n = 6-9$ for (B) and (C)].

analysis revealed that CD4⁺ T cells infiltrated the affected ureteral tissues (Fig. 5A). They were detected frequently between collagen laid fibrotic areas in the adventitia and epithelium areas together with Gr-1⁺ granulocytic cells. Many of these T cells were Th17, Th1, IL-10⁺ T cells, and Foxp3⁺ T cells (Fig. 5B, Supplemental Fig. 2B, 2C). These effector and regulatory T cells appeared in draining lymph nodes, kidneys, and ureters at similar time points (Supplemental Fig. 2C). When C2 water was switched to regular water at 4 wk, C2RD at 6 wk was significantly suppressed (Fig. 6A). This indicates that mice may recover from subterminal C2RD, and prolonged exposure up to 6 wk is necessary to maximize C2RD development. Von Kossa staining did not reveal any ureteral stones (not shown). Thus, increased concentrations of C2 for prolonged time periods develop inflammatory responses and hyperplasia in UPJ and proximal ureter tissues leading to ureteral obstruction.

Other SCFAs such as C3 and C4 can also induce C2RD

We investigated also the effect of other SCFAs such as C3 and C4 on the renal system. Oral administration of these SCFAs at 200 mM

(the same as for C2) in drinking water reproducibly induced the renal disease (Fig. 6B). Increased numbers of Th17, Th1, and IL-10⁺ T cells were found in the draining lymph node, kidney, and ureteral tissues of C3- or C4-fed mice (Fig. 6C). In a manner similar to C2-induced disease, C3 and C4 induced hydronephrosis and hyperplasia in kidney and ureter tissues, respectively (Fig. 6D). The histological changes in the kidneys and ureters in these mice were almost indistinguishable from those administered with C2. Hence, all major SCFAs have the C2RD-inducing activity.

T cells are required for C2RD development

Because Th17 and Th1 cells expand in numbers in C2RD and can mediate tissue inflammation in the renal system (30, 31), we investigated the role of T cells in C2RD development. To determine the role of T cells in C2RD, we fed TCR $\alpha\beta$ T cell-deficient C57BL/6 mice with C2 for 6 wk. Most T cell-deficient mice did not develop C2RD unlike wild-type mice (Fig. 7A), indicating a critical role for T cells in C2RD development.

We next determined whether T cell cytokines such as IL-17A and IFN- γ play any role in the pathogenesis of C2RD. We employed

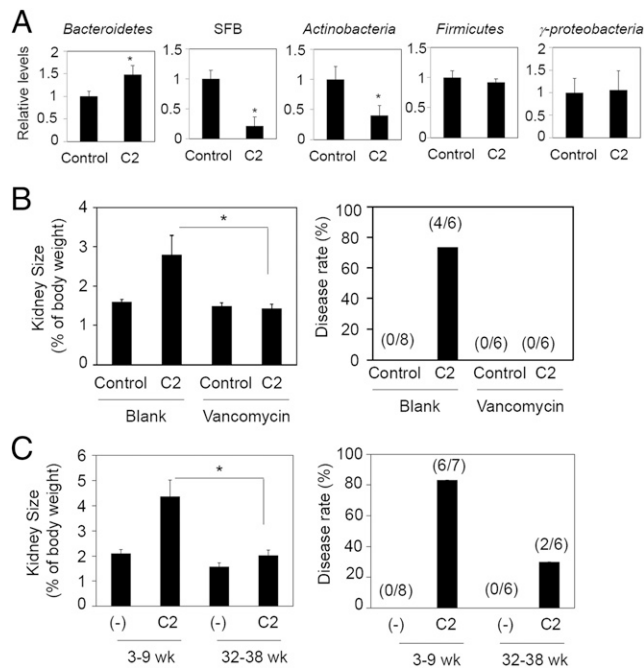


FIGURE 9. Impact of microbiota and age on C2RD development. **(A)** Mice were fed C2 water for 6 wk, and the relative levels of selected microbiota groups were determined by quantitative PCR of group-specific 16S rRNA sequences. **(B)** Mice were fed C2 together with vancomycin for 6 wk, and C2RD development was assessed. **(C)** Mice were on C2 water from 3 or 32 wk of age for 6 wk for the assessment of C2RD development. Gross tissue appearance, disease rate, and relative kidney weight are shown. Representative or pooled data are shown [$n = 6-8$ for (A)–(C)]. Error bars are SEM. * $p \leq 0.05$ from control groups by Student t test (paired two-tailed).

neutralizing Abs to IL-17A and IFN- γ . These neutralizing Abs were highly effective in preventing C2RD (Fig. 7B). Both Abs were effective in decreasing the frequencies of Th1, Th17, and IL-10 $^{+}$ T cells in kidney tissues (Fig. 7C).

We further studied whether C2RD development requires GPR41 and GPR43, two major receptors for C2, C3, and C4. It has been reported that GPR41 and GPR43 were expressed at low levels in kidneys (32). Our data indicate that *Gpr41* and *Gpr43* mRNAs were expressed in kidney or ureteral tissues, but compared with that of colon, their expression levels were very low (Fig. 8A). Mice deficient in *Gpr41* or *Gpr43* were susceptible to C2RD, and no difference was found between wild-type and the two SCFA receptor-deficient mice in disease rate, relative kidney weight, and T cell cytokine phenotype (Fig. 8B, 8C). These data indicate that the two SCFA receptors are dispensable for C2RD development.

Impact of gut microbiota and age on C2RD development

Because gut bacteria and host responses can affect each other, we examined the levels of major bacterial groups in C2-fed mice (Fig. 9A). Bacteroidetes were enriched but the levels of segmented filamentous bacteria and Actinobacteria were decreased in C2RD mice. Because of these changes in microbiota, we fed mice with C2 along with vancomycin to suppress the effect of microbiota. Vancomycin, which effectively suppresses Bacteroidetes and Firmicutes (33), completely prevented C2RD development (Fig. 9B). UPJ obstruction in humans is more prevalent in early versus late life (34). We examined C2RD development in young (C2 administration started at 3 wk of age) versus older (started at 32 wk) mice. The old mice were more resistant to C2RD development than were the young mice (Fig. 9C). Thus, C2RD development in mice is age-dependent.

SCFAs hyperactivate the mTOR pathway and induce inflammatory T cells in the renal system

The mTOR pathway plays a critical role not only in regulating renal disease development but also in T cell differentiation (35), and its activity is increased by SCFAs in T cells in a GPR41- or GPR43-independent manner (9). SCFAs may activate the mTOR pathway to generate inflammatory T cells in the renal system to cause C2RD. We examined whether SCFAs activate the mTOR pathway in renal lymph node T cells. SCFAs efficiently induced rS6 phosphorylation in renal lymph node CD4 $^{+}$ T cells (Fig. 10A). The rS6 phosphorylation in renal lymph node CD4 $^{+}$ T cells was completely abolished by rapamycin. We next examined whether SCFAs facilitate the generation of inflammatory T cells from kidney-draining lymph node T cells. SCFAs greatly increased the generation of Th1 and Th17 cells from the culture of total lymph node cells, which were obtained through digestion of whole lymph nodes with collagenase to retain potentially important accessory cells of the renal system (Fig. 10B). Again, rapamycin completely suppressed the promoting effect of SCFAs on Th1 or Th17 cells. We next studied whether SCFAs activate the mTOR pathway in renal T cells in vivo. Kidney CD4 $^{+}$ T cells in C2-treated mice had increased rS6 phosphorylation compared with their control counterparts in a rapamycin-dependent manner (Fig. 10C). Rapamycin effectively suppressed C2RD development (Fig. 10D) and blocked the increased generation of Th17 and Th1 cells in the kidneys of C2-fed mice (Fig. 10E). These data indicate that the mTOR pathway plays a key role in the development of inflammatory T cells and C2RD pathogenesis in response to C2.

Discussion

In this study, we examined the effects of elevated levels of SCFAs on tissue inflammation in the renal system. Orally administered SCFAs increased Th1 and Th17 cells in ureter and kidney tissues and induced a renal disease, which we termed C2RD, where UPJ-proximal ureter tissue develops inflammation and severe hyperplasia, resulting in kidney hydronephrosis. This reveals the potentially inflammatory function of elevated levels of SCFAs.

A key feature of C2RD pathogenesis is the T cell-mediated inflammatory response. C2RD development was effectively suppressed by $\alpha\beta$ T cell deficiency, suggesting an essential role for T cells in mediating the disease. This rules out the possibility that C2RD is simply induced by a toxic or necrotic effect of SCFAs on the renal system. T cells produce IFN- γ , IL-17, and other effector molecules, central for tissue inflammation in renal tissues (31, 36, 37). We found that SCFAs promote the generation of T cells producing IFN- γ and IL-17 in the ureter, kidney, and draining lymph nodes. IFN- γ and IL-17 are functionally important, as their neutralization suppressed C2RD development. Although the numbers of regulatory T cells, including IL-10 $^{+}$ T cells and Foxp3 $^{+}$ T cells, were also increased in C2RD, this did not correlate with suppressed immune responses. Rather, the increased numbers of regulatory T cells along with Th1 and Th17 cells indicate generally increased T cell responses in C2RD. Whereas the increased numbers of regulatory T cells were not sufficient to rein in the overall inflammatory response in C2RD, these cells have the potential to suppress inflammation in appropriate conditions. In this regard, SCFAs may affect underlying renal diseases and even play a protective role in the renal system. For example, a protective effect of C2 was observed on ischemia-induced acute kidney disease, where a C2 solution was injected i.p. just before injury (32).

Rapamycin has been used to treat certain renal diseases in animals and humans (38, 39). We demonstrated that rapamycin

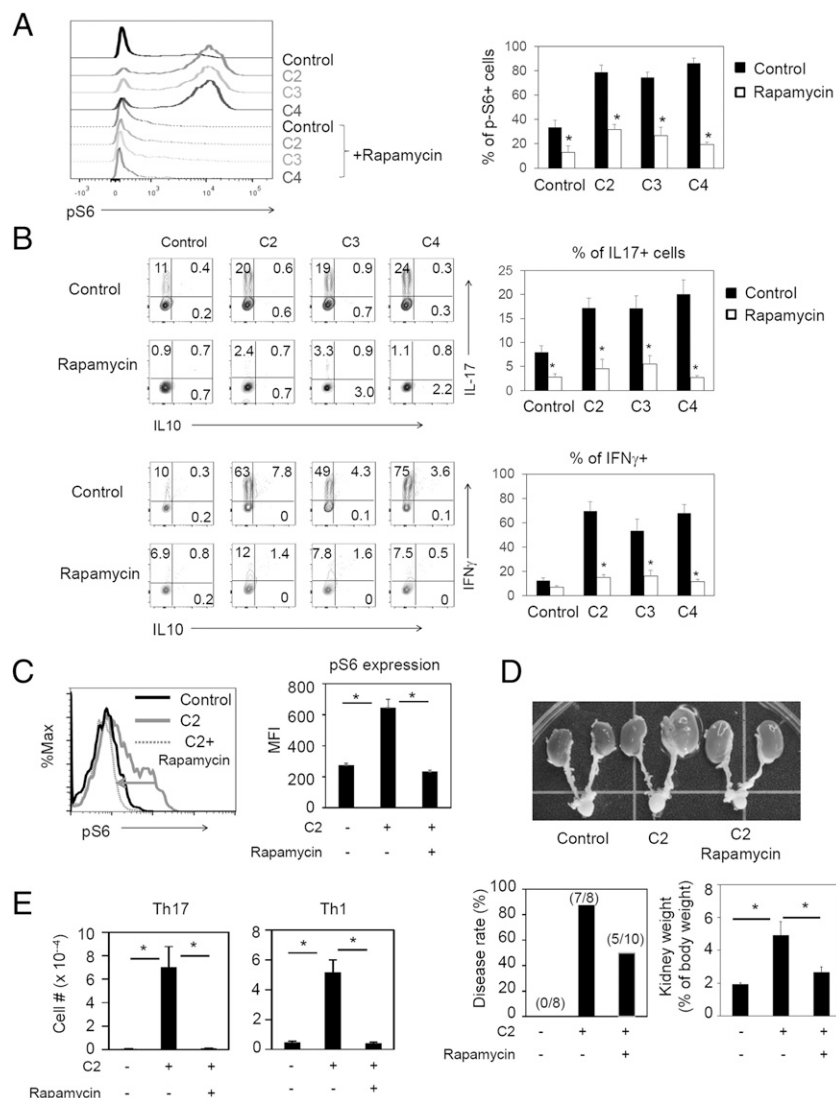


FIGURE 10. Rapamycin suppressed C2RD and the generation of inflammatory T cells by SCFAs. (A) Impact of SCFAs and rapamycin on mTOR activity based on rS6 phosphorylation in renal lymph node T cells in culture. Total renal lymph node cells were cultured with SCFAs in a Tnp condition. (B) Generation of Th1 and Th17 cells in response to SCFAs in vitro. Total renal lymph node cells were cultured with SCFAs and/or rapamycin in a Th1 or Th17 condition. Impacts of C2 and rapamycin on mTOR activation (C), C2RD development (D), and generation of Th17 and Th1 cells (E) in vivo are shown. Mice were fed with C2 and rapamycin in drinking water. Representative or pooled data are shown [$n = 4$ for (A) and (B), $n = 7-10$ for (C)–(E)]. pS6⁺ cells (A and C) and Th17 or Th1 cells (B and C) were gated on CD4⁺ cells. Error bars are SEM. * $p \leq 0.05$ from control or between indicated groups by Student t test (paired two-tailed).

completely suppressed C2RD. Rapamycin suppresses the mTOR pathway important for T cell differentiation into cytokine-producing effector T cells such as Th1 and Th17 cells. In addition to T cells, activation of the mTOR pathway in tissue cells is important for development of renal diseases (39, 40). Thus, although our data identified T cells as a primary target for rapamycin in C2RD, we do not rule out the possibility that rapamycin works through other cell types. Whereas the function of SCFAs in activating the mTOR pathway is important, we found no role for GPR41 and GPR43 in C2RD development. Along with T cells, the numbers of dendritic cells were increased in the inflamed tissues of C2RD mice. SCFAs regulate dendritic cell maturation and function in a manner dependent on SCFA receptors or HDAC inhibition (15–17). In this regard, the induction of proinflammatory cytokine IL-23 in dendritic cells by C4 is linked to its role as a HDAC inhibitor for epigenetic modification of genes (17).

UPJ or ureteral obstruction in humans is induced by a number of reasons, from developmental malformation to urolithiasis and inflammatory ureteral obstruction. Also, mutations in certain genes induce hydronephrosis in animals and humans (41–43). It is interesting that orally administered SCFAs can also induce UPJ obstruction. In C2RD, ureters undergo gradual inflammation and obstruction during a 2- to 6-wk period in response to oral ad-

ministration of microbial metabolites. UPJ obstruction in humans is at least twice as prevalent in males as in females (44, 45). Chronic kidney diseases with end-stage renal diseases are also more prevalent in males (40). Another interesting feature of C2RD is that 3-wk-old animals are more susceptible than are 6-mo-old mice. In this regard, C2RD development is highly similar to UPJ obstruction in humans. Artificial UUO models (46), although very useful to study the pathological consequence of ureteral obstruction in kidney tissues, are not ideal to study disease-initiating inflammatory processes in ureters. C2RD appears to be a good model to study inflammation in the ureter even before the development of ureteral obstruction and kidney tissue injury. The pathological features of C2RD also make it a good model to study the inflammatory process in kidney tissues following ureteral obstruction.

C2RD is induced by C2 at 150 mM or higher after at least 4 wk of continued exposure. It is unlikely that C2RD is readily induced by physiologically produced SCFAs in the gut. Our results should not be interpreted as evidence that naturally produced or consumed SCFAs cause C2RD. Rather, our results indicate that SCFAs have the potential to induce tissue inflammation when their levels are chronically elevated. It is a question of interest why SCFAs specifically induce inflammation in the renal system. SCFAs affect T cells also in other tissues such as the spleen and intestine. In the

steady-state without apparent immune responses, SCFAs promote the generation of IL-10-producing, but not inflammatory, T cells (5). However, during inflammatory conditions, SCFAs increase Th1 and Th17 cells as well (5). Although we found no evidence that C2 at physiologically relevant concentrations following C2 administration has toxic or inflammatory effects on ureter or kidney tissue cells in vitro, it is possible that increased SCFAs exert such effects in vivo in renal tissue-specific milieus. Moreover, renal tissues appear to concentrate C2 during oral administration, which could make the cells of the renal system relatively more sensitive to SCFAs.

We observed that the gut microbiota were altered by C2 and required for C2RD development. The changes in gut microbiota, increased Bacteroidetes but decreased segmented filamentous bacteria and Actinobacteria levels, could be a cause for as well as the result of the inflammation. Chronic inflammatory diseases, including kidney diseases, autoimmune demyelination, arthritis, and colitis, are ameliorated when the gut microbiota are suppressed by antibiotics or in germ-free conditions (47–51). Perhaps similar mechanisms are behind the attenuated inflammatory responses in C2RD and other inflammatory diseases. Potential mechanisms include dysbiosis-associated low-grade inflammatory responses or adjuvant effects of commensal bacteria and their products in inducing inflammatory responses in the renal system. Moreover, altered microbiota can lead to increased production of endotoxins and uremic toxins, which is linked to decreased kidney function (52, 53).

In summary, SCFAs, when chronically increased in vivo, generate Th1 and Th17 cells, which induce tissue inflammation in ureteral tissues. The SCFA-induced inflammatory activity causes ureteral obstruction and hydronephrosis. We conclude that SCFAs have the potential to generate inflammatory T cells for induction of tissue inflammation.

Acknowledgments

We thank S. Hashimoto-Hill, M. Kim, and L. Friesen (Purdue University) for assistance in carrying out this study.

Disclosures

The authors have no financial conflicts of interest.

References

- Cummings, J. H., E. W. Pomare, W. J. Branch, C. P. Naylor, and G. T. Macfarlane. 1987. Short chain fatty acids in human large intestine, portal, hepatic and venous blood. *Gut* 28: 1221–1227.
- Donohoe, D. R., N. Garge, X. Zhang, W. Sun, T. M. O'Connell, M. K. Bunger, and S. J. Bultman. 2011. The microbiome and butyrate regulate energy metabolism and autophagy in the mammalian colon. *Cell Metab.* 13: 517–526.
- Xiong, Y., N. Miyamoto, K. Shibata, M. A. Valasek, T. Motoike, R. M. Kedzierski, and M. Yanagisawa. 2004. Short-chain fatty acids stimulate leptin production in adipocytes through the G protein-coupled receptor GPR41. *Proc. Natl. Acad. Sci. USA* 101: 1045–1050.
- Pluznick, J. L., R. J. Protzko, H. Gevorgyan, Z. Peterlin, A. Sipos, J. Han, I. Brunet, L. X. Wan, F. Rey, T. Wang, et al. 2013. Olfactory receptor responding to gut microbiota-derived signals plays a role in renin secretion and blood pressure regulation. *Proc. Natl. Acad. Sci. USA* 110: 4410–4415.
- Park, J., M. Kim, S. G. Kang, A. H. Jannasch, B. Cooper, J. Patterson, and C. H. Kim. 2015. Short-chain fatty acids induce both effector and regulatory T cells by suppression of histone deacetylases and regulation of the mTOR-S6K pathway. *Mucosal Immunol.* 8: 80–93.
- Kim, M. H., S. G. Kang, J. H. Park, M. Yanagisawa, and C. H. Kim. 2013. Short-chain fatty acids activate GPR41 and GPR43 on intestinal epithelial cells to promote inflammatory responses in mice. *Gastroenterology* 145: 396–406.e1–10. doi:10.1053/j.gastro.2013.04.056
- Thangaraju, M., G. A. Cresci, K. Liu, S. Ananth, J. P. Gnanaprakasam, D. D. Browning, J. D. Mellinger, S. B. Smith, G. J. Digby, N. A. Lambert, et al. 2009. GPR109A is a G-protein-coupled receptor for the bacterial fermentation product butyrate and functions as a tumor suppressor in colon. *Cancer Res.* 69: 2826–2832.
- Hecker, M., N. Sommer, H. Voigtman, O. Pak, A. Mohr, M. Wolf, I. Vadasz, S. Herold, N. Weissmann, R. E. Morty, et al. 2014. Impact of short- and medium-chain fatty acids on mitochondrial function in severe inflammation. *J. Parenter. Enteral Nutr.* 38: 587–594.
- Kim, C. H., J. Park, and M. Kim. 2014. Gut microbiota-derived short-chain fatty acids, T cells, and inflammation. *Immune Netw.* 14: 277–288.
- Arpaia, N., C. Campbell, X. Fan, S. Dikly, J. van der Veeken, P. deRoos, H. Liu, J. R. Cross, K. Pfeffer, P. J. Coffey, and A. Y. Rudensky. 2013. Metabolites produced by commensal bacteria promote peripheral regulatory T-cell generation. *Nature* 504: 451–455.
- Smith, P. M., M. R. Howitt, N. Panikov, M. Michaud, C. A. Gallini, M. Bohlooly-Y, J. N. Glickman, and W. S. Garrett. 2013. The microbial metabolites, short-chain fatty acids, regulate colonic Treg cell homeostasis. *Science* 341: 569–573.
- Furusawa, Y., Y. Obata, S. Fukuda, T. A. Endo, G. Nakato, D. Takahashi, Y. Nakanishi, C. Uetake, K. Kato, T. Kato, et al. 2013. Commensal microbe-derived butyrate induces the differentiation of colonic regulatory T cells. *Nature* 504: 446–450.
- Soldavini, J., and J. D. Kaunitz. 2013. Pathobiology and potential therapeutic value of intestinal short-chain fatty acids in gut inflammation and obesity. *Dig. Dis. Sci.* 58: 2756–2766.
- Vaziri, N. D., S. M. Liu, W. L. Lau, M. Khazaeli, S. Naztehrani, S. H. Farzaneh, D. A. Kieffer, S. H. Adams, and R. J. Martin. 2014. High amylose resistant starch diet ameliorates oxidative stress, inflammation, and progression of chronic kidney disease. *PLoS One* 9: e114881.
- Trompette, A., E. S. Gollwitzer, K. Yadava, A. K. Sichelstiel, N. Sprenger, C. Ngom-Bru, C. Blanchard, T. Junt, L. P. Nicod, N. L. Harris, and B. J. Marsland. 2014. Gut microbiota metabolism of dietary fiber influences allergic airway disease and hematopoiesis. *Nat. Med.* 20: 159–166.
- Singh, N., A. Gurav, S. Sivaprakasam, E. Brady, R. Padia, H. Shi, M. Thangaraju, P. D. Prasad, S. Manicassamy, D. H. Munn, et al. 2014. Activation of Gpr109a, receptor for niacin and the commensal metabolite butyrate, suppresses colonic inflammation and carcinogenesis. *Immunity* 40: 128–139.
- Berndt, B. E., M. Zhang, S. Y. Owyang, T. S. Cole, T. W. Wang, J. Luther, N. A. Veniaminova, J. L. Merchant, C. C. Chen, G. B. Huffnagle, and J. Y. Kao. 2012. Butyrate increases IL-23 production by stimulated dendritic cells. *Am. J. Physiol. Gastrointest. Liver Physiol.* 303: G1384–G1392.
- Corraliza, I. M., M. L. Campo, G. Soler, and M. Modolell. 1994. Determination of arginase activity in macrophages: a micromethod. *J. Immunol. Methods* 174: 231–235.
- Goergen, C. J., H. H. Li, U. Francke, and C. A. Taylor. 2011. Induced chromosome deletion in a Williams-Beuren syndrome mouse model causes cardiovascular abnormalities. *J. Vasc. Res.* 48: 119–129.
- Kang, S. G., J. Park, J. Y. Cho, B. Ulrich, and C. H. Kim. 2011. Complementary roles of retinoic acid and TGF- β 1 in coordinated expression of mucosal integrins by T cells. *Mucosal Immunol.* 4: 66–82.
- Barman, M., D. Unold, K. Shifley, E. Amir, K. Hung, N. Bos, and N. Salzman. 2008. Enteric salmonellosis disrupts the microbial ecology of the murine gastrointestinal tract. *Infect. Immun.* 76: 907–915.
- Young, J. H., M. J. Klag, P. Muntner, J. L. Whyte, M. Pahor, and J. Coresh. 2002. Blood pressure and decline in kidney function: findings from the Systolic Hypertension in the Elderly Program (SHEP). *J. Am. Soc. Nephrol.* 13: 2776–2782.
- Iliescu, R., and J. F. Reckelhoff. 2008. Sex and the kidney. *Hypertension* 51: 1000–1001.
- Kurts, C., U. Panzer, H. J. Anders, and A. J. Rees. 2013. The immune system and kidney disease: basic concepts and clinical implications. *Nat. Rev. Immunol.* 13: 738–753.
- Chung, A. C., and H. Y. Lan. 2011. Chemokines in renal injury. *J. Am. Soc. Nephrol.* 22: 802–809.
- Wu, B., and J. D. Brooks. 2012. Gene expression changes induced by unilateral ureteral obstruction in mice. *J. Urol.* 188: 1033–1041.
- Becknell, B., A. R. Carpenter, J. L. Allen, M. E. Wilhide, S. E. Ingraham, D. S. Hains, and K. M. McHugh. 2013. Molecular basis of renal adaptation in a murine model of congenital obstructive nephropathy. *PLoS One* 8: e72762.
- Pandey, P., S. Qin, J. Ho, J. Zhou, and J. A. Kreidberg. 2011. Systems biology approach to identify transcriptome reprogramming and candidate microRNA targets during the progression of polycystic kidney disease. *BMC Syst. Biol.* 5: 56.
- Reddy, P. S., H. M. Legault, J. P. Sypek, M. J. Collins, E. Goad, S. J. Goldman, W. Liu, S. Murray, A. J. Dorner, and M. O'Toole. 2008. Mapping similarities in mTOR pathway perturbations in mouse lupus nephritis models and human lupus nephritis. *Arthritis Res. Ther.* 10: R127.
- Hopfer, H., J. Holzer, S. Hünemörder, H.-J. Paust, M. Sachs, C. Meyer-Schwesinger, J.-E. Turner, U. Panzer, and H.-W. Mittrücker. 2012. Characterization of the renal CD4⁺ T-cell response in experimental autoimmune glomerulonephritis. *Kidney Int.* 82: 60–71.
- Dong, X., L. A. Bachman, M. N. Miller, K. A. Nath, and M. D. Griffin. 2008. Dendritic cells facilitate accumulation of IL-17 T cells in the kidney following acute renal obstruction. *Kidney Int.* 74: 1294–1309.
- Andrade-Oliveira, V., M. T. Amato, M. N. Correa-Costa, A. Castoldi, R. J. Felizardo, D. C. de Almeida, E. J. Bassi, P. M. Moraes-Vieira, M. I. Hyane, and A. C. Rodas. 2015. Gut bacteria products prevent AKI induced by ischemia-reperfusion. *J. Am. Soc. Nephrol.* 26: 1877–1888.
- Rea, M. C., A. Dobson, O. O'Sullivan, F. Crispie, F. Fouhy, P. D. Cotter, F. Shanahan, B. Kiely, C. Hill, and R. P. Ross. 2011. Effect of broad- and narrow-spectrum antimicrobials on *Clostridium difficile* and microbial diversity in a model of the distal colon. *Proc. Natl. Acad. Sci. USA* 108(Suppl. 1): 4639–4644.
- Lam, J. S., A. Breda, and P. G. Schulam. 2007. Ureteropelvic junction obstruction. *J. Urol.* 177: 1652–1658.

35. Lieberthal, W., and J. S. Levine. 2009. The role of the mammalian target of rapamycin (mTOR) in renal disease. *J. Am. Soc. Nephrol.* 20: 2493–2502.
36. Timoshanko, J. R., S. R. Holdsworth, A. R. Kitching, and P. G. Tipping. 2002. IFN- γ production by intrinsic renal cells and bone marrow-derived cells is required for full expression of crescentic glomerulonephritis in mice. *J. Immunol.* 168: 4135–4141.
37. Xue, L., K. Xie, X. Han, Z. Yang, J. Qiu, Z. Zhao, and T. Bao. 2011. Detrimental functions of IL-17A in renal ischemia-reperfusion injury in mice. *J. Surg. Res.* 171: 266–274.
38. Wu, M. J., M. C. Wen, Y. T. Chiu, Y. Y. Chiou, K. H. Shu, and M.-J. Tang. 2006. Rapamycin attenuates unilateral ureteral obstruction-induced renal fibrosis. *Kidney Int.* 69: 2029–2036.
39. Chen, G., H. Chen, C. Wang, Y. Peng, L. Sun, H. Liu, and F. Liu. 2012. Rapamycin ameliorates kidney fibrosis by inhibiting the activation of mTOR signaling in interstitial macrophages and myofibroblasts. *PLoS One* 7: e33626.
40. Iseki, K., C. Iseki, Y. Ikemiya, and K. Fukiyama. 1996. Risk of developing end-stage renal disease in a cohort of mass screening. *Kidney Int.* 49: 800–805.
41. Weiss, R. M., S. Guo, A. Shan, H. Shi, R.-A. Romano, S. Sinha, L. G. Cantley, and J.-K. Guo. 2013. Brg1 determines urothelial cell fate during ureter development. *J. Am. Soc. Nephrol.* 24: 618–626.
42. Kim, S. T., S.-Y. Ahn, W. Swat, and J. H. Miner. 2014. DLG1 influences distal ureter maturation via a non-epithelial cell autonomous mechanism involving reduced retinoic acid signaling, Ret expression, and apoptosis. *Dev. Biol.* 390: 160–169.
43. Murer, L., F. Addabbo, M. Carmosino, G. Procino, G. Tamma, G. Montini, W. Rigamonti, P. Zucchetta, M. Della Vella, A. Venturini, et al. 2004. Selective decrease in urinary aquaporin 2 and increase in prostaglandin E₂ excretion is associated with postobstructive polyuria in human congenital hydronephrosis. *J. Am. Soc. Nephrol.* 15: 2705–2712.
44. Woodward, M., and D. Frank. 2002. Postnatal management of antenatal hydronephrosis. *BJU Int.* 89: 149–156.
45. Stern, J. M., S. Park, J. K. Anderson, J. Landman, M. Pearle, and J. A. Cadeddu. 2007. Functional assessment of crossing vessels as etiology of ureteropelvic junction obstruction. *Urology* 69: 1022–1024.
46. Chevalier, R. L., M. S. Forbes, and B. A. Thornhill. 2009. Ureteral obstruction as a model of renal interstitial fibrosis and obstructive nephropathy. *Kidney Int.* 75: 1145–1152.
47. Taurog, J. D., J. A. Richardson, J. T. Croft, W. A. Simmons, M. Zhou, J. L. Fernández-Sueiro, E. Balish, and R. E. Hammer. 1994. The germfree state prevents development of gut and joint inflammatory disease in HLA-B27 transgenic rats. *J. Exp. Med.* 180: 2359–2364.
48. Rath, H. C., M. Schultz, R. Freitag, L. A. Dieleman, F. Li, H. J. Linde, J. Schölmerich, and R. B. Sartor. 2001. Different subsets of enteric bacteria induce and perpetuate experimental colitis in rats and mice. *Infect. Immun.* 69: 2277–2285.
49. Maldonado, M. A., V. Kakkanaiah, G. C. MacDonald, F. Chen, E. A. Reap, E. Balish, W. R. Farkas, J. C. Jennette, M. P. Madaio, B. L. Kotzin, et al. 1999. The role of environmental antigens in the spontaneous development of autoimmunity in MRL-*lpr* mice. *J. Immunol.* 162: 6322–6330.
50. Hallman, T. M., M. Peng, R. Meade, W. W. Hancock, M. P. Madaio, and D. L. Gasser. 2006. The mitochondrial and kidney disease phenotypes of *kd/kd* mice under germfree conditions. *J. Autoimmun.* 26: 1–6.
51. Berer, K., M. Mues, M. Koutrosos, Z. A. Rasbi, M. Boziki, C. Johner, H. Wekerle, and G. Krishnamoorthy. 2011. Commensal microbiota and myelin autoantigen cooperate to trigger autoimmune demyelination. *Nature* 479: 538–541.
52. Lin, C. J., H. H. Chen, C. F. Pan, C. K. Chuang, T. J. Wang, F. J. Sun, and C. J. Wu. 2011. p-Cresylsulfate and indoxyl sulfate level at different stages of chronic kidney disease. *J. Clin. Lab. Anal.* 25: 191–197.
53. McIntyre, C. W., L. E. Harrison, M. T. Eldehni, H. J. Jefferies, C. C. Szeto, S. G. John, M. K. Sigrist, J. O. Burton, D. Hothi, S. Korsheed, et al. 2011. Circulating endotoxemia: a novel factor in systemic inflammation and cardiovascular disease in chronic kidney disease. *Clin. J. Am. Soc. Nephrol.* 6: 133–141.